Structure and Phase Behavior of Self-Assembled DPPC−DNA−Metal Cation Complexes

Michela Pisani,[†] Paolo Bruni,[†] Giulio Caracciolo,[‡] Ruggero Caminiti,[‡] and Oriano Francescangeli*[,§]

Dipartimento di Scienze dei Materiali e della Terra, Università Politecnica delle Marche, Via Brecce Bianche, I-60131 Ancona, Italy, Dipartimento di Chimica, Università 'La Sapienza', P.le A. Moro 5, 00185 Roma, Italy, and Dipartimento di Fisica e Ingegneria dei Materiali e del Territorio, Università Politecnica delle Marche, Via Brecce Bianche, I-60131 Ancona, Italy

Received: May 3, 2006; In Final Form: May 12, 2006

Multilamellar liposomes of dipalmitoylphosphatidylcholine (DPPC) in solution with DNA and bivalent metal cations (Ca^{2+}, Mn^{2+}, Mg^{2+}) self-assemble into a ternary DPPC−DNA−Me^{2+} complex. The supramolecular structure of the complex consists of an ordered multilamellar assembly where hydrated DNA helices are sandwiched between the lipid bilayers and the metal cations bind the phosphate groups of DNA to the lipid polar heads. In the range of explored incubation times, the complex coexists with the uncomplexed DPPC over the whole temperature range investigated (20−55 °C). Accordingly, two distinct coexisting lamellar phases are observed, one corresponding to the ternary complex and the other to the uncomplexed lipid. The structure and thermotropic phase behavior of both of these have been investigated by means of synchrotron X-ray diffraction, and the relevant structural data are deduced from experimental electron density profiles. While the uncomplexed lipid exhibits the same phase behavior as pure DPPC, that is, $L_{\beta'}-P_{\beta'}-L_{\alpha}$, the thermotropic behavior of the bound lipid in the complex is partially altered. This is manifested as an increase in the main transition temperature and the disappearance of the ripple phase leading to the single $L^{c}_{\beta'}-L^{c}_{a}$ phase transition. The role of the different metal cations in promoting and stabilizing the DNA condensation into the ternary complex is also discussed.

Introduction

Interaction between lipids and DNA has become an active area of research in recent years due to fundamental and applicative interests. Lipids in water self-assemble into lamellar bilayers, which comprise the basic structural elements of biomembranes.[1] The supramolecular packing of the bilayers forms lyotropic liquid crystals (LCs) that display richness of phase behavior and structures. On the other hand, the ability of DNA to influence the structure of biomembranes and to initiate polymorphic phase transitions in bilayers may have important biological implications.[2,3]

Cationic lipids can easily form stable complexes with DNA owing to the attraction forces between the opposite net charges of the lipid and the DNA.[4−10] Complexes composed of cationic liposomes (self-closed lipid vesicles) and DNA have been shown to be promising nonviral delivery systems for applications in gene therapy, due to their ability to mimic natural viruses as chemical carriers of extracellular DNA across the cell and nuclear membranes (transfection).[11−14] However, their transfer efficiency is still relatively low compared to that of viral vectors, one of the reasons being the instability of a cationic liposome (CL)−DNA complex in the presence of serum in vivo.[15] Tremendous effort has been devoted to solving this problem, including the continuous synthesis of new cationic lipids and the search for new formulations that exhibit reduced interactions with serum proteins.[15,16] Also, CLs are frequently toxic for the cells. These principal drawbacks are presently stimulating scientists to focus major efforts toward a better understanding of the structure−activity relationships with the ultimate goal of enabling a design-based approach to delivery.

Complexes composed exclusively of neutral (zwitterionic) lipids offer an alternative to CLs, in that they exhibit lower inherent cytotoxicity,[17,18] much longer circulation lifetimes, and very different clearance profiles.[19] Within this frame, some of the present authors have recently studied ternary complexes formed by the self-assembled association of neutral liposomes (L's), DNA, and bivalent metal cations in water solutions.[20,21] Different from CLs, the interaction between the neutral lipid and DNA is mediated by the metal cations that act as a bridge between the phosphate groups of DNA and the zwitterionic lipid headgroups. L−DNA−Me^{2+} complexes having different microstructures that reflect the structure and phase symmetry of the parent pure lipids were prepared, using different unsaturated neutral liposomes [namely, dioleoylphosphatidylcholine (DOPC), dilinoleoylphosphatidylcholine (DLPC), and dioleoylphosphatidylethanolamine (DOPE)], different DNA (from calf thymus, salmon sperma, and λ-phage), and bivalent metal cations (Mn^{2+}, Mg^{2+}, Ca^{2+}, Co^{2+}, Fe^{2+}).[20−23] The microscopic structure was probed on the nanometer scale by means of synchrotron X-ray diffraction (XRD).[20,22−25] It was found that the DOPC−DNA−Me^{2+} and DLPC−DNA−Me^{2+} complexes exhibit the liquid-crystalline L^{c}_{α} phase (c stands for complex) consisting of the multilamellar aggregation of stacked alternating lipid bilayers and hydrated DNA monolayers.[20,21] Differently, solutions of

* Corresponding author. Phone: +39 0712204734. Fax: +39 0712204729. E-mail: o.francescangeli@univpm.it.

[†] Dipartimento di Scienze dei Materiali e della Terra, Università Politecnica delle Marche.

[‡] Università 'La Sapienza'.

[§] Dipartimento di Fisica e Ingegneria dei Materiali e del Territorio, Università Politecnica delle Marche.

10.1021/jp062713v CCC: $33.50
Published on Web 06/14/2006

DOPE and bivalent metal cations were found to condense DNA into an inverse hexagonal structure, H_{II}^{c}, in which the lipids are regularly packed in a 2D hexagonal lattice, with the DNA strands filling the cylindrical water gaps.[26] More recently, the self-assembly of the L_{α}^{c} phase was demonstrated in the ternary complexes DOPC−DNA−Me^{2+} (Me = Ca and Mn) using plasmid instead of linear DNA.[27] In fact, it is generally believed that the native supercoiled form of the plasmid DNA is the *physiologically active* conformation and hence preferably used in transfection processes. Also, an attempt of an in vitro transfection has been reported,[27] which shows the capability of these complexes to transfect DNA. On the basis of these results, efficient encapsulation of DNA plasmids in these ternary neutral complexes may represent an important alternative to current systemic gene approaches.

Aimed at providing a deeper insight into the structure−function correlations of these systems, we have recently extended the study to the ternary complexes L−DNA−Me^{2+} in which the neutral liposome has fully saturated hydrocarbon chains. Saturated chains are very flexible, and when in a nonfrozen state, they can exhibit a large number of conformations due to the complete rotational freedom of each single bond, leading to a variety of mesophases. In particular, hydrated samples of fully saturated phosphatidylcholine derivatives can exist in one of the relevant four bilayer phases: a crystalline (L_c) phase formed on equilibrium at low temperatures in which the alkyl chains are packed on an orthorhombic lattice; a gel ($L_{\beta'}$) phase in which the fully extended chains, packed on a quasihexagonal lattice, are tilted with respect to the layer normal; a ripple ($P_{\beta'}$) phase in which the lipid bilayer is distorted by a periodic ripple characterized by a two-dimensional monoclinic lattice; and a conventional liquid-crystal (L_{α}) phase in which the chains are melted.[28]

In this paper, we report the study of the structure and phase behavior of self-assembled dipalmitoylphosphatidylcholine (DPPC)−DNA−Me^{2+} complexes prepared from different DNA (namely, from calf thymus and plasmid) and metal cations (Ca^{2+}, Mn^{2+}, Mg^{2+}). DPPC plays an important role within the wide class of saturated liposomes because of its widespread application in molecular biology and biomembrane system modeling.[1] The mesomorphic behavior of DPPC is also reasonably well understood, with recent papers detailing its structure in both the gel and fluid phases.[29−31] It has been shown that, in the presence of DNA and Ca^{2+}, multilamellar liposomes of DPPC when in excess form a multilamellar complex in which DNA is embedded between the DPPC layers.[32,33] This complex exhibits rich phase behavior, with a two-phase DPPC region and also interesting thermotropic mesomorphism. Recently, a highly ordered arrangement of DNA within a DPPC−DNA−Ca^{2+} complex prepared from unilamellar vesicles has been reported.[34]

The purpose of the present investigation is to study the effect of divalent metal cations such as Ca^{2+}, Mn^{2+}, and Mg^{2+} on the structure and phase behavior of the DPPC−DNA−Me^{2+} complexes formed in a self-assembled manner from multilamellar vesicles in excess water. The richest phase behavior of DPPC compared to previously studied liposomes gives us the further opportunity of investigating to which extent the structure and phase behavior of the pure parent lipids are transferred into the complex upon condensation. This is a point of great general interest, even though only marginally addressed so far, not only for fundamental implications but mainly in view of a future design-based approach to gene delivery.

Experimetal Methods

Materials and Sample Preparation. DNA from calf thymus was purchased from Sigma Chemical Co. The DNA aqueous solution (8 mg/mL) was sonicated in order to induce a DNA fragmentation whose length distribution, detected by gel electrophoresis, varied between 500 and 2000 bp. The plasmid pGreenLantern I was prepared according to the following procedure. Plasmid pGreenLantern I was propagated in transformed *Escherichia coli* cells. *E coli* cells were grown in standard Luria Bertani medium at pH 7.0. Cells were harvested by centrifugation, and the plasmid DNA was extracted and purified using a Qiagen Plasmid Maxi Kit (Qiagen, Santa Clarita, CA) following the manufacturer's recommended protocols. In brief, the plasmid purification procedure involved alkaline lysis of the cells and isolation of the plasmid by binding it in an anion exchange resin. The concentration of the purified plasmid preparation was determined using a UV−visible spectrophotometer (SpectraMax Plus, Molecular Devices, Sunnyvale, CA) using OD260 (optical density at a wavelength of 260 nm). Standard agarose gel electrophoresis on a 1 % wt/wt agarose gel was conducted to investigate the plasmid structural integrity and revealed two bands. The high-mobility band was attributed to the most compact or supercoiled form of plasmid DNA. The other band with low mobility indicated the overall nonsupercoil content in the plasmid preparation. The purified plasmid was predominantly composed of the supercoiled form. The final concentration of plasmid DNA was 1 mg/mL.

The metal ions Ca^{2+}, Mn^{2+}, and Mg^{2+}, as chloride, were purchased from Sigma Chemical Co. DPPC was purchased from Avanti Polar Lipids and used without purification. DPPC was dissolved in chloroform and the solvent removed in a stream of nitrogen; the sample was then maintained under a vacuum for 5 h in order to remove any trace of solvent. To operate under physiological conditions, a HEPES buffer (20 mM, pH 7.2) was added to the dried film to reach the final concentration 13.6 mg/mL. The lipid solution was incubated at 50 °C for 2 h, above the melting temperature, and it was vortexed several times during the hydration period. Liposome solutions were stored at 4 °C. The triple complexes for the XRD experiments were prepared by mixing equal volumes of the solutions of DPPC, DNA, and metal. The samples were prepared at different relative molar ratios of the three components DPPC/DNA/Me^{2+}, with the concentration of DNA being expressed in moles per nucleotide. After a short incubation time (a few hours) at room temperature (RT), the complex was transferred into a 1 mm glass capillary for the X-ray diffraction measurements. In a few selected cases, longer incubation times of the samples were adopted (up to 1 week), for the purposes of investigation of the kinetics of the complexation process. The complexes prepared with plasmid DNA are more dilute than those preparedwith DNA from calf thymus (DPPC 1.6 mg/mL, DNA 1 mg/1 mL, Me^{2+} ∼1 mg/1 mL).

X-ray Diffraction Measurements. Small-angle X-ray scattering (SAXS) measurements were carried out at the high-brilliance beamline ID2 at the European Synchrotron Radiation Facility (Grenoble, France). The energy of the incident beam was 12.5 keV (λ = 0.995 Å), the beam size was 100 μm, and the sample-to-detector distance was 1.2 m. The diffraction patterns were collected by a 2D CCD detector. We investigated the q range from q_{min} = 0.4 nm^{-1} to q_{max} = 5 nm^{-1} with a resolution of 5×10^{-3} nm^{-1} (fwhm). The sample was held in a 1-mm-sized glass capillary. Measurements were performed in the temperature range 25−55 °C. To avoid radiation damage, a maximum exposure time of 3 s/frame was used for any given

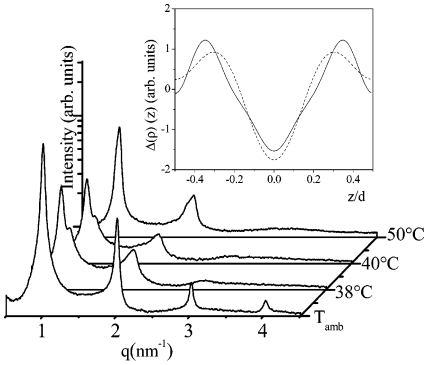

Figure 1. SAXS patterns of the DPPC liposome solution in excess water as a function of temperature. The inset shows the electron density profile along the normal to the bilayers in both the gel $L_{\beta'}$ (continuous line) and the liquid-crystalline L_α (dotted line) phases.

sample. Satisfactory statistics were attained by repeating several measurements on fresh samples. The collected 2D powder diffraction spectra were angularly integrated to get 1D intensity versus q patterns. These data were then corrected for the detector efficiency, empty sample holder, and HEPES bulk solution. To calculate the electron density, the integrated intensities (I) of the diffraction peaks were determined by fitting the data with Lorentzian line shapes using a nonlinear baseline. The electron density profile ($\Delta\rho$), along the normal to the bilayers (z), was then calculated as a Fourier sum

$$\Delta\rho = \frac{\rho(z) - \langle\rho\rangle}{[\langle\rho^2(z)\rangle - \langle\rho\rangle^2]^{1/2}} = \sum_{l=1}^{N} F_l \cos\left(2\pi l \frac{z}{d}\right) \qquad (1)$$

where $\rho(z)$ is the electron density, $\langle\rho\rangle$ is its average value, N is the highest order of the fundamental reflection observed in the SAXS patterns, F_l is the form factor of the (00l) reflection, d is the thickness of the repeating unit (including one lipid bilayer and one water layer), and the origin of the z axis is chosen in the middle of the lipid bilayer. The form factors (F_l) in eq 1 were calculated as the square root of the corresponding integrated intensities (I_l) corrected for the Lorentz factor. The phase problem was solved by means of a pattern recognition approach based on the histogram of the electron density map,[35] and the results were found to be in agreement with those obtained with different approaches.[36,37]

The synchrotron SAXS data were integrated with wide-angle X-ray scattering (WAXS) measurements carried out by means of an in-house diffractometer equipped with the Bruker AXS general area detector diffraction system (GADDS) using monochromatic Cu Kα radiation ($\lambda = 1.54$ Å).

Results and Discussion

First, we studied as a reference sample the pure DPPC lipid solution in excess water. On increasing temperature, we observed the well-known mesophase sequence

$$L_{\beta'} \xrightarrow{34\ ^\circ\mathrm{C}} P_{\beta'} \xrightarrow{41.3\ ^\circ\mathrm{C}} L_\alpha$$

Figure 1 shows selected SAXS patterns in the investigated temperature range between 25 and 55 °C. The lamellar repeat distance (d spacing) is $d = 6.27$ nm in the $L_{\beta'}$ phase (at 30 °C), $d = 7.02$ nm in the $P_{\beta'}$ phase (at 38 °C), and $d = 6.47$ nm in the L_α phase (50 °C). These values are consistent with the literature values for DPPC in water solution.[30,38,39] The electron density profile along the normal to the bilayers in both the gel ($L_{\beta'}$) and the liquid-crystalline (L_α) phase are shown in the inset of Figure 1. The lamellar repeat distance is the sum of the membrane (bilayer) thickness (d_m) and the water space between the bilayers (d_w). The distance d_{HH} between the two electron density maxima corresponding to the phospholipid headgroups gives a good estimate of the bilayer thickness. The value obtained in the $L_{\beta'}$ phase is $d_{HH} = 4.34$ nm, from which the thickness of the water gap is estimated as $d_w = d - d_{HH} = 1.93$ nm, while for the L_α phase it is $d_{HH} = 3.92$ nm and hence $d_w = 2.55$ nm.

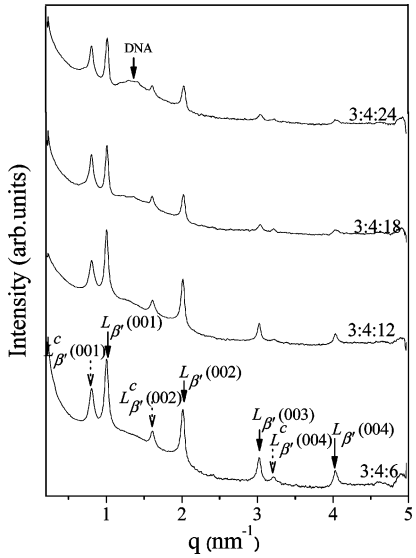

Figure 2. Room temperature SAXS patterns of the DPPC−DNA−Ca^{2+} complex as a function of calcium concentration, at a DPPC/DNA mole ratio of 3:4.

XRD measurements of the DPPC−DNA−Me^{2+} complexes were carried out on a wide range of molar ratios of the components and, for any fixed composition, as a function of temperature. Figure 2 shows the room temperature (RT) SAXS patterns of DPPC−DNA−Ca^{2+} at different calcium concentrations with the DPPC/DNA molar ratio fixed at 3:4. These patterns exhibit two distinct sets of peaks, labeled as $L^c_{\beta'}$ and $L_{\beta'}$, that can be indexed on a 1D lattice with different unit cell spacings, namely, $d_c = 7.91$ nm and $d = 6.40$ nm (independently calculated as $d = 2\pi d/q$, with n being the order of the Bragg peak). This experimental evidence points to the coexistence of two DPPC lamellar phases: the $L^c_{\beta'}$ phase of the DPPC−DNA−Ca^{2+} complex, with lamellar repeat distance d_c and the $L_{\beta'}$ phase of the uncomplexed DPPC, with lamellar repeat distance d. We identify these as the same two phases earlier observed[3,40] by differential scanning calorimetry (DSC) and temperature scanning ultrasound. The structure of the $L^c_{\beta'}$ phase consists of stacks of alternating lipid bilayers and DNA monolayers, with the amphiphilic molecules being in the gel state. The DNA strands are sandwiched between the lipid bilayers and are bound to these by the metal cations. More specifically, the formation of the triple complex is promoted by the fusogenic action of the positively charged metal ions that bind the polar heads of DPPC with the negatively charged phosphate groups of DNA, similarly to what already observed for the L_α phase of DOPC−DNA−Me^{2+} complexes.[20] On the other hand, the lamellar $L_{\beta'}$ phase of the uncomplexed DPPC preserves the same structure as that in pure DPPC, with only a slight change of the lattice spacing. Apart from the lamellar peaks, the SAXS scans exhibit also a much broader and weaker minimum that becomes well evident at higher Ca^{2+} concentrations (above 3:4:12). This signal (labeled DNA in Figure 2) arises from the in-layer DNA−DNA correlations and corre-

sponds to an average interchain distance of 4.7 nm calculated as $d_{DNA} = 2\pi/q_{DNA}$. Whereas the presence of this peak is quite common in complexes with cationic liposomes,[4−7] it was never observed in the many DOPC−DNA−Me^{2+} and DLPC−DNA−Me^{2+} complexes previously studied by our group under the same preparation conditions, even after longer incubation times (up to 1 week). Therefore, the presence of this peak in the present complexes is remarkable and suggests a specific role of the DPPC liposome with fully saturated hydrocarbon chains. In particular, the onset of the short-range chain correlations may arise from the good packing and rather slow motion of the hydrocarbon chains in the gel state of the $L_{\beta'}$ phase, which favors a better organization of the DNA chains during condensation within the lipid bilayers. This hypothesis is supported by the SAXS measurements at higher temperature (shown later), which clearly show how the DNA−DNA correlation peak is progressively reduced on increasing temperature until it completely disappears in the liquid-crystalline (fluid) phase L_α where greater disorder and chain mobility work against DNA ordering.

Similar SAXS patterns (not shown here) were observed for the ternary complexes with Mg^{2+} and Mn^{2+}, under the same preparation and experimental conditions. Only slight differences were observed, mainly concerned with the relative intensity of the two sets of peaks associated with the two lamellar (complexed and uncomplexed) phases. This in particular proves the role of chemical species of the metal cation on the formation kinetics of the ternary complex. In fact, the volume fraction of the mixture occupied by each of the two lamellar phases ($L^c_{\beta'}$ and $L_{\beta'}$) is proportional to the integrated intensity (I_1) of the corresponding first-order diffraction peak. Accordingly, the ratio $R = I_1(L^c_{\beta'})/[I_1(L^c_{\beta'}) + I_1(L_{\beta'})]$ is a measure of the relative amount of the starting lipid solution that undergoes complexation. In previous studies on unsaturated L−DNA−Me^{2+} complexes,[20−22,26] also confirmed by the present study on selected samples submitted to longer annealing at RT before measurements, we found a continuous growth of R on increasing incubation time until a saturation value (R_{sat}) was reached, corresponding to the onset of thermodynamic equilibrium of the two coexisting phases. Under our experimental conditions of an excess of metal cations, we found $R_{sat} \approx 1$, corresponding to the complete transformation of the starting lipid into the complex aggregate. However, the kinetics of the process is rather slow at room temperature, involving incubation times from a few days up to several weeks, depending on the preparation conditions and the physicochemical parameters of the lipid solution mixture. That is the reason we observed coexistence of the two lamellar phases after incubation times of the order of a few hours. On the basis of these considerations, the values of R at different incubation times measured for complexes with different cations (under identical experimental conditions) simply reflect the role of the chemical species on the kinetics of the complexation process. The experimental data for Ca^{2+} give R values 1 order of magnitude larger than those for Mn^{2+} or Mg^{2+} complexes and prove the stronger fusogenic action of Ca^{2+} compared to the other cations. As an example of the behavior of the DPPC−DNA−Mg^{2+} complex, Figure 3 shows the SAXS pattern of the 3:4:24 mixture after an incubation time of 8 h at room temperature. Only after such incubation the pattern exhibits well appreciable features of the complex including the DNA−DNA correlation peak. The higher fusogenic strength reflects the greater potency of Ca^{2+} in the physicochemical mechanisms involved in the complexation process. In fact, it is well-known that the permeability of hydrated ions within the lipid bilayers depends on the ionic size

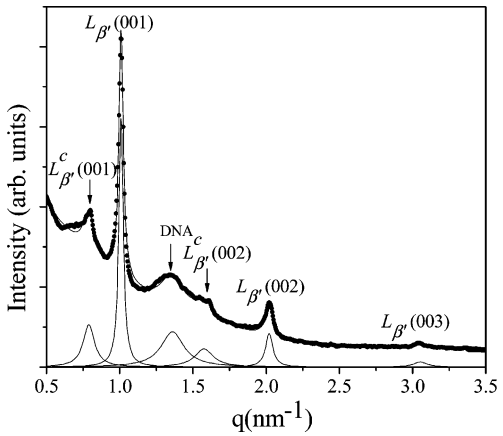

Figure 3. Room temperature SAXS pattern of the DPPC−DNA−Mg^{2+} complex at a molar ratio of 3:4:24 after an incubation time of 8 h at room temperature. The continuous line shapes are the components of the diffracted signal after background subtraction.

and the level of hydration, and the literature data[41] set Ca^{2+} as the most permeable among the divalent metal ions. Nevertheless, the order of association constants of metal ions with the phosphate group of phosphatidylcholine (PC), which decreases according to $Zn^{2+} > Cu^{2+} > Ca^{2+} > Mg^{2+}$ for divalent cations,[42] as well as the sequence of the intrinsic binding constants of alkaline-earth metal cations onto PC membranes,[43] $Ca^{2+} > Mg^{2+} > Sr^{2+} > Ba^{2+}$, are in agreement with the observed effects.

Coexistence of complexed and uncomplexed lipid phases in DPPC−DNA−Ca^{2+} complexes from multilamellar vesicles was previously observed by McManus et al.,[33,34] only under the condition of an excess of lipid, in particular at DNA/lipid mole ratios above 1:8. However, we have observed the two-phase coexistence over a wider range of relative molar ratios including the case of an excess of either DNA or metal cations. These apparently different results, however, do not contradict each other simply because they refer to samples under different experimental conditions. In fact, in refs 33 and 34, the authors investigated the samples after incubation times of the order of 1 week that should correspond to the onset of thermodynamic equilibrium. Under these conditions, the $L_{\beta'} \rightarrow L^c_{\beta'}$ phase transformation has completed and therefore coexistence is observed only in an excess of lipid.

Figure 4 shows the behavior of the lamellar repeat distances (d) of both $L^c_{\beta'}$ and $L_{\beta'}$ phases as a function of the metal cation concentration for a DPPC/DNA ratio fixed at 3:4. No regular trend is observed for the d spacing of the $L^c_{\beta'}$ phase, which remains essentially constant over the investigated range of metal concentration. In particular, the DPPC−DNA−Mg^{2+} complex exhibits a value of $d \sim 8.0$ nm, slightly higher than that measured for the complexes with Mn^{2+} or Ca^{2+}, $d \sim 7.9$ nm. The constancy of d for the phase $L^c_{\beta'}$ of DPPC−DNA−Ca^{2+} over the investigated range of metal concentration is consistent with the results of McManus et al.[33] in similar samples studied in an excess of lipid. In fact, with a DNA/lipid molar ratio of 1:8, they found a minimum of d (corresponding to the most compact structural arrangement of the bilayers) at a Ca^{2+} concentration of 5 mM. Under these conditions, in fact, the stoichiometry ratio suggests that the calcium bridges adjacent lipids and forms an effective cationic moiety, which then binds to DNA. On further increasing the metal concentration, they found an increase in the lamellar repeat distance tending to approach a limiting value of 8.0 nm, which is reached however only under our experimental conditions of an excess of metal.

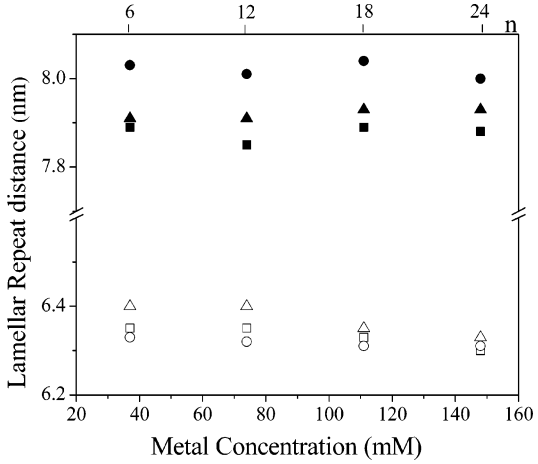

Figure 4. Lamellar repeat distance for complexed and uncomplexed lipid at room temperature as a function of metal concentration. Full symbols are associated to the triple complexes DPPC−DNA−Me^{2+} [Mn (■), Mg (●), Ca (▲)]), and open symbols represent uncomplexed DPPC lipid [Mn (□), Mg (○), Ca (△)].

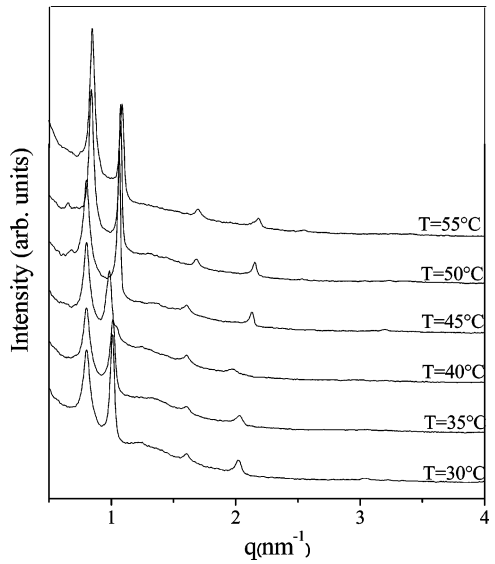

Figure 5. Synchrotron XRD patterns of the DPPC−DNA−Ca^{2+} complex prepared at a 3:4:24 molar ratio as a function of temperature.

Once this saturation value is reached, no further increase of *d* is observed on increasing the metal concentration, which has been exactly observed here. Different from the bound lipid, in our complexes, the lamellar *d* spacing of the unbound lipid shows a regular continuous reduction on increasing metal ion concentration, which is more pronounced for Ca^{2+} and Mn^{2+}. This behavior of the uncomplexed lipid fraction is again in agreement with the results of ref 33 and also with our previous results on DOPC−DNA−Me^{2+} complexes.[20−22]

We have investigated the thermotropic phase behavior of the complexes in the temperature range between 20 and 55 °C, well above the main transition temperature (i.e., the transition to the fluid L_α phase) of the pure lipid, $T_m = 41.3$ °C. Figures 5 and 6 show selected SAXS patterns of DPPC−DNA−Ca^{2+} and DPPC−DNA−Mn^{2+} (3:4:24), respectively, measured at different temperatures in the relevant thermal range. For the DPPC−DNA−Mg^{2+} mixture, we have observed a behavior quite similar to that of Figure 5. Two important conclusions can thus be drawn. First, for all samples, the coexistence of complexed and uncomplexed lipid lamellar phases persists over the entire explored thermal range. Nevertheless, a comparison of Figures 5 and 6 evidences for the Mn^{2+} sample a stronger

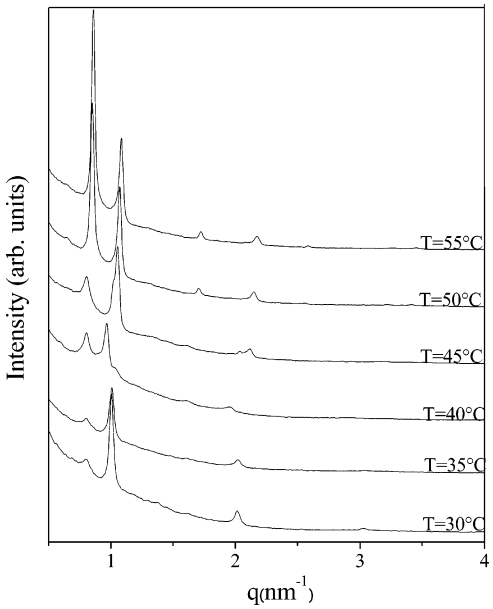

Figure 6. Synchrotron XRD patterns of the DPPC−DNA−Mn^{2+} complex prepared at a 3:4:24 molar ratio as a function of temperature.

effect of the temperature on the relative concentrations of the coexisting lamellar phases. Increasing the temperature was previously known to favor the kinetics of complex formation in the fluid L_α phase,[21] and this effect is obviously amplified when temperature increase produces a transition from the gel to the fluid phase, as occurs in our samples. In fact, higher thermal energy means higher chain mobility which favors the mechanism of complex formation by promoting intercalation of DNA chains between the lipid bilayers. This effect becomes manifest in all of the investigated samples through the continuous growth of the diffraction peaks of the complex on increasing temperature. In the Mn^{2+} and Mg^{2+} mixtures, this temperature effect is strongly enhanced near the transition from the gel to the fluid phase because of the previously discussed slower condensation kinetics of these complexes in the gel phase, compared to the complexes with Ca^{2+}.

The second point concerns the thermotropic behavior of the complex and in particular the extent to which the phase sequence and structure of the pure parent lipid is transferred into the complex upon condensation. In previous papers, we have found a close correspondence between the phase structure of the pure lipid and that of the related complex, both for lamellar (DOPC and DLPC)[20−22] and hexagonal (DOPE)[26] phases. In the present DPPC-based complexes, such correspondence appears to be still strong yet not fully achieved. In fact, while pure DPPC forms the ripple phase $P_{\beta'}$ between the gel and liquid-crystalline states,[31,44−46] also confirmed by our measurements on the reference DPPC solution, this does not appear to be the case for the complex. The ripple phase in DPPC is believed to occur as an intermediate in the transition of the tail portion of the lipids from a tilted configuration in the gel phase to a perpendicular conformation in the LC state. Information on its structure is usually obtained from WAXS data or by SAXS data collected from aligned samples. We studied the ripple phase by combining the lamellar *d* spacing versus temperature synchrotron data with complementary WAXS measurements (at lower resolution) carried out by means of the in-house diffractometer. Figure 7 shows the lamellar repeat distance versus temperature data for uncomplexed (empty symbols) and bound (full symbols) liposomes in the complex with different metal cations. Figure 8A shows the WAXS pattern of the DPPC−

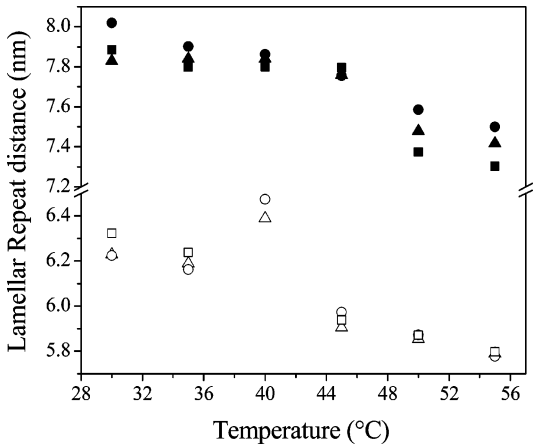

Figure 7. Lamellar repeat distance as a function of temperature for DPPC−DNA−Me^{2+} samples with different metal cations (Me = Ca, Mn, Mg). Open symbols are for the uncomplexed DPPC lipid [Mn (□), Mg (○), Ca (△)]; full symbols are for the complexed DPPC [Mn (■), Mg (●), Ca (▲)].

DNA−Mn^{2+} complex (3:4:24) collected at different temperatures in the relevant mesophasic range, after a 1 week incubation time when the complexation process has completed and only the $L^c_{\beta'}$ is present. For the sake of comparison, Figure 8B shows a similar scan on the reference DPPC sample. These patterns are shown after correction for the background contribution (sample holder and HEPES bulk solution). Under these conditions, the wide-angle features observed in Figure 8A can be entirely attributed to the $L^c_{\beta'}$ phase of the complex. The wide-angle feature of the DPPC $L_{\beta'}$ phase (RT pattern of Figure 8B) exhibits a relatively sharp peak superimposed with a broadened peak at higher q values.[47] The former is centered around 14.8 nm^{-1} ($d = 2\pi/q = 0.42$ nm), and the latter arises from powder averaging of the (1,1) reflection of a distorted hexagonal lattice with chains tilted toward the next neighbors.[48,49] Occurrence of the ripple phase $P_{\beta'}$ on increasing temperature above ∼34 °C is manifested by the modification of the WAXS pattern into a single symmetric peak, again centered at 14.8 nm^{-1} (see Figure 8B, $T = 40$ °C). The peak symmetry indicates that the lipid chains are packed on a regular hexagonal lattice.[48,49] This peak, however, is considerably broader than that corresponding to conventional L_β phases formed in planar bilayers, reflecting the tilt of the chains in the $P_{\beta'}$ phase. At higher temperatures, the pattern of the L_α phase (Figure 8B, $T = 50$ °C), as would be expected, consists of a single broad diffuse reflection. Consistent with this mesophase sequence, the experimental lamellar d spacing of the pure DPPC increases (from $d = 6.27$ nm to $d = 7.02$ nm) across the first transition $L_{\beta'} \rightarrow P_{\beta'}$ and then decreases to $d = 63.5$ nm across the second transition $P_{\beta'} \rightarrow L_\alpha$. A similar trend of the d spacing is observed in the unbound lipid fraction of the complexes for all of the metal cations investigated (Figure 7). This confirms that the thermotropic phase transitions of the uncomplexed lipid within the complex are the same as pure DPPC, in agreement with previous results in the same ternary mixtures but in an excess of lipid.[33] Combining our results with those of ref 33, therefore, suggests that preserving the thermotropic behavior of the pure lipid is a general feature of the bound lipid in these ternary complexes. The reduced lamellar d spacing of each single phase ($L_{\beta'}$, $P_{\beta'}$, L_α) of the unbound lipid compared to the corresponding phase of the pure lipid, an effect remarkably strong in the fluid L_α phase, can indeed be ascribed to the action of the metal cations that, due to ion transport across membranes, penetrate the internal layers within the multilamellar vesicle structure and bind to the polar heads of the lipids. A partial explanation of this d reduction is that the pressure exerted by the bound lipid phase at high calcium concentrations as it swells slightly may "squeeze" the lamellae of the complex.[33] This fact alone, however, does not account for the magnitude of the

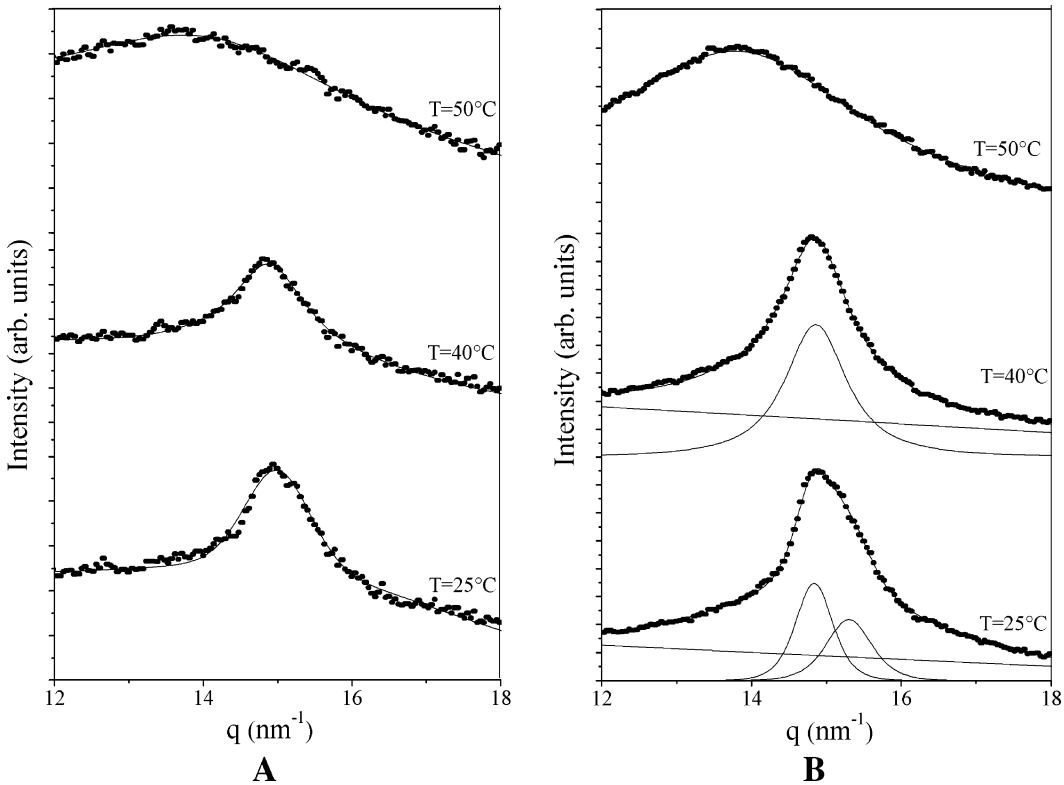

Figure 8. (A) WAXS pattern of the DPPC−DNA−Mn^{2+} complex (3:4:24) collected at different temperatures in the relevant mesophasic range, after an incubation time of 1 week. (B) WAXS pattern of a pure DPPC sample at different temperatures.

decrease in the fluid phase. Another possibility has been suggested by McManus et al.,[33] based on a theory of Rouzina and Blomfield,[50] that predicts macroion attraction due to electrostatic correlation between screening counterions (at a small separation on planar surfaces) in the DPPC surfaces with bound calcium.

Contrary to the observations of the uncomplexed lipid, no modification of the WAXS pattern is observed in the complex on increasing temperature up to the transition to the fluid phase. The two patterns reported in Figure 8A at temperatures of 25 and 40 °C are quite similar, and the same situation is observed throughout the whole range from RT up to the main transition temperature. The WAXS peak of the complex below the main transition temperature is similar to the analogous peak of the RT pattern of pure DPPC, even though its asymmetry on the high-q side is less pronounced. This allows the low-temperature phase of the complex to be identified as the lamellar $L^c_{\beta'}$ phase. For a more detailed description of the structure, however, we should consider that the commonly labeled ordered $L_{\beta'}$ phase consists in fact of three two-dimensional phases differentiated by the direction of chain with respect to the in-plane lattice:[51] (1) $L_{\beta I}$, with tilt toward the nearest neighbor; (2) $L_{\beta F}$, tilt between next neighbor; (3) $L_{\beta L}$, tilt at intermediate directions. On the basis of solely the present data, it is not possible to state whether the asymmetry reduction of the complex peak, compared to pure DPPC, is due simply to a smaller tilt angle of the chains in the $L_{\beta F}$ phase, or more likely the $L^c_{\beta'}$ phase is actually a combination of different orientations of the tilt. High-resolution XRD on oriented samples is necessary to clarify this point. On the basis of the WAXS data, therefore, the complex exhibits a single thermotropic phase transition $L^c_{\beta'} \rightarrow L^c_a$, with no evidence of the ripple phase. This is confirmed by the data of Figure 7 (full symbols) that, different from the corresponding data for the unbound lipid, show a continuous and regular slight decrease up to the main transition where a far greater change occurs. The conclusion is that the presence of DNA and metal cations inhibits the formation of the ripple phase in the complex, as previously observed in similar complexes but in an excess of lipid.[33] This suggests that, on binding the cations to the polar headgroups, the movements of the lipid bilayers become restricted and this prevents the bilayers from the natural "kinking" associated with the onset of the ripple phase. This finding is also in agreement with a previous paper[52,53] where an analogous effect of inhibition of the ripple phase by DNA was found in complexes from mixtures of neutral dimyristoylphosphatidylcholine (DMPC) and cationic dimyristoyltrimethylammonium-propane (DMTAP) lipids.

A further relevant effect of DNA on the thermotropic behavior of the complex, compared to that of the pure lipid, is manifested by the shift of the main transition toward higher temperatures, which is in agreement with previous observations.[3,40] From the data of Figure 7, the main transition temperature (T_m) of the complex lies between 45 and 50 °C, well above the T_m value of the pure lipid (T_m = 41.3 °C) and also above the same complex when in an excess of lipid (T_m = 43.1 °C).[33] A systematic increase of the main transition temperature due to the effect of DNA complexation was found also in zwitterionic−cationic DMPC−DMTAP mixtures.[53] Even though the mechanism of complexation in neutral and cationic lipids is different, the observed increase of T_m seems to be a general feature of DNA−lipid complexes. This effect naturally originates from the stabilizing action of the lipid chains promoted by the binding interactions, either direct or mediated by metal cations, between the negatively charged phosphate groups of DNA and the polar lipid headgroups.

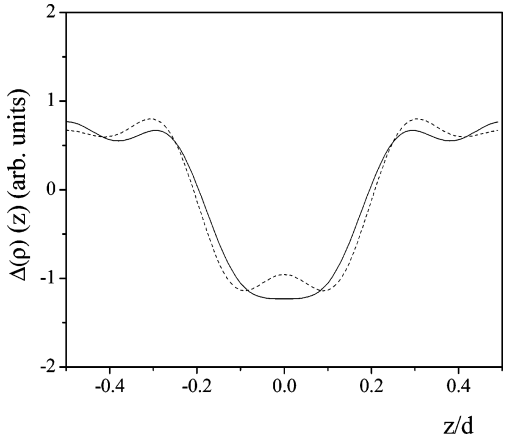

Figure 9. Electron density profile along the normal to the bilayer for the ternary complex DPPC−DNA−Ca^{2+} at 30 °C in the $L_{\beta'}$ phase (continuous line) and at 55 °C in the L_α phase (dotted line).

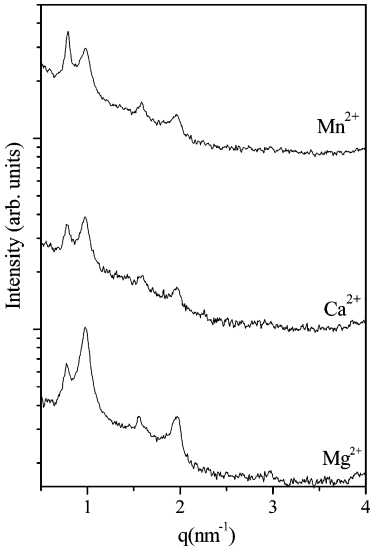

Figure 10. Room temperature SAXS pattern of the DPPC−DNA-(plasmid)−Me^{2+} complex (Me = Ca, Mn, Mg) at a molar ratio of 3:4:12.

As an example of the structural data of the bilayers, the lamellar spacing in the $L^c_{\beta'}$ phase of DPPC−DNA−Ca^{2+} at 30 °C is d = 7.83 nm, whereas in the $L_{\beta'}$ phase of the uncomplexed lipid it is d = 6.23 nm. At 55 °C in the fluid L_α phase, d = 7.42 nm in the L^c_α phase of the complex and d = 5.79 nm in the L_α phase of the unbound lipid. Figure 9 shows the calculated electron density profile, along the normal to the bilayers, of both the $L^c_{\beta'}$ phase (at 30 °C) and the L^c_α phase (at 55 °C) of the DPPC−DNA−Ca^{2+} complex. The relevant structural parameters extracted from the electron density map are d_{HH} = 4.60 nm and d_w = 3.23 nm for the $L^c_{\beta'}$ phase and d_{HH} = 4.52 nm and d_w = 2.89 nm for the L^c_α phase. On the basis of these data, the water gaps d_w = 3.23 nm and d_w = 2.89 nm in the $L^c_{\beta'}$ and L^c_α phases, respectively, leave sufficient space (within the experimental errors) to accommodate between the bilayers one DNA strand (≅2 nm) plus two hydrated Ca^{2+} ions (≅1 nm) that bridge the DNA phosphate groups to the polar heads of the lipids, in agreement with the proposed structural model.

We have studied also the structure and the phase behavior of the triple DPPC−DNA−Me^{2+} complex with plasmid DNA instead of linear DNA. The interest in the characterization of

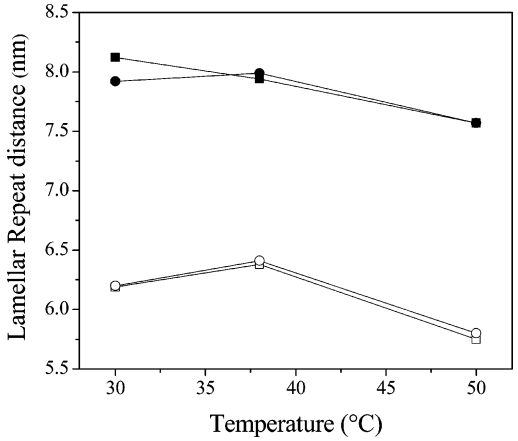

Figure 11. Lamellar repeat distance vs temperature for both uncomplexed lipid (open symbols) and lipid complexed with DNA (solid symbols). Squares refer to mixtures with DNA from calf thymus, whereas circles refer to mixtures with DNA plasmid.

these systems arises from the native supercoiled form of the plasmid DNA, which is the physiologically active conformation and hence preferably used in transfection processes.[54] Examples of the XRD patterns of the triple complexes DPPC−DNA(plasmid)−Me^{2+} at a molar ratio of 3:4:12 with different metal cations (Me^{2+} = Mg, Ca, Mn) are shown in Figure 10. All of the main features previously discussed for the complexes with linear DNA are still present, even though the broadening of the diffraction peak compared to those of linear DNA is a distinctive sign of the less ordered layer structuring. This is mostly due to the greater difficulty of assembling the supercoiled form of the plasmid into the planar layering of the lamellar structure. The trend of the *d* spacing as a function of temperature for the lamellar phases of both complexed and uncomplexed lipid fraction is shown in Figure 11. For the sake of comparison, the corresponding data for similar complexes with linear DNA at the same temperatures are reported. Consistent with the previous results for complexes with linear DNA, comparison between the two sets of data (of complex and unbound lipid) confirms the absence of the ripple phase in the complex.

Conclusion

DPPC multilamellar liposomes in solution with DNA (both linear and plasmid) and bivalent metal cations (Ca^{2+}, Mn^{2+}, Mg^{2+}) self-assemble into a ternary DPPC−DNA−Me^{2+} complex. The supramolecular structure of the complex consists of an ordered multilamellar assembly where hydrated DNA helices are sandwiched between the lipid bilayers and the metal cations bind the phosphate groups of DNA to the lipid polar heads. Among the investigated cations, Ca^{2+} has been found as the most effective in promoting the formation process of the complex.

In the range of incubation times investigated, the DPPC−DNA−Me^{2+} complex coexists with the uncomplexed DPPC lipid over the relevant temperature range explored. Accordingly, two distinct lamellar phases are observed within the same aggregate, one corresponding to the ternary complex and the other to the uncomplexed lipid. While the uncomplexed lipid exhibits the same thermotropic phase behavior as pure DPPC, that is, $L_{\beta'}-P_{\beta'}-L_{\alpha}$, the mesomorphic behavior of the bound lipid in the complex is partially altered. This is manifested as the disappearance of the ripple phase and a remarkable increase in the main transition temperature: the observed thermotropic phase sequence of the complex reduces to $L^{c}_{\beta'}-L^{c}_{a}$. The relevant structural parameters of both $L^{c}_{\beta'}$ and L^{c}_{a} lamellar phases, deduced from the experimental electron density profiles, are in agreement with the proposed structural model.

Acknowledgment. The authors acknowledge Dr. Thomas Weiss and Dr. T. Narayanan of the experimental staff of ID02 at ESRF for technical support. This work was financially supported by the grant Cofin-2004 n.2004033543_002 of the Italian Ministero dell'Istruzione, dell'Università e della Ricerca.

References and Notes

(1) Lasic, D. D. *Liposomes: from Physics to Applications*; Elsevier: Amsterdam, The Netherlands, 1993.
(2) Sternberg, B.; Sorgi F. L.; Huang L. *FEBS Lett.* **1994**, *356*, 361.
(3) Tarahovski, Y. S.; Khusainova, R. S.; Gorelov, A. V.; Nicolaeva, T. I.; Deev, A. A.; Dawson, A. K.; Ivanitsky, G. R. *FEBS Lett.* **1996**, *390*, 133.
(4) Rädler, J. O.; Koltover, I.; Salditt, T.; Safinya, C. R. *Science* **1997**, *275*, 810.
(5) Salditt, T.; Koltover, I.; Rädler, J. O.; Safinya, C. R. *Phys. Rev. Lett.* **1997**, *79*, 2582.
(6) Salditt, T.; Koltover, I.; Rädler, J. O.; Safinya, C. R. *Phys. Rev. E* **1998**, *58*, 889.
(7) Koltover, I.; Salditt, T.; Rädler, J. O.; Safinya, C. R. *Science* **1998**, *281*, 78.
(8) Artzner, F.; Zantl, R.; Rapp, G.; Rädler, J. O. *Phys. Rev. Lett.* **1998**, *81*, 5015.
(9) Caracciolo, G.; Caminiti, R.; Pozzi, D.; Friello, M.; Boffi, F.; Congiu Castellano, A. *Chem. Phys. Lett.* **2002**, *351*, 222.
(10) Caracciolo, G.; Pozzi, D.; Caminiti, R.; Congiu Castellano, A. *Eur. Phys. J.* **2003**, *E10*, 331
(11) Felgner, P. L.; Gradeck, T. R.; Holm, M.; Roman, R.; Chan, H. W.; Wenz, M.; Northrop, J. P.; Ringold, G. M.; Danielson, M. *Proc. Natl. Acad. Sci. U.S.A.* **1987**, *84*, 7413.
(12) Hofland, H. E. J.; Shepard, L.; Sullivan, S. M. *Proc. Natl. Acad. Sci. U.S.A.* **1996**, *93*, 7305.
(13) Spector, M. S.; Schnur, J. M. *Science* **1997**, *275*, 7.
(14) Lasic, D. D.; Strey, H.; Stuart, M. C. A.; Podgornik, R.; Frederick, P. M. *J. Am. Chem. Soc.* **1997**, *119*, 832.
(15) Chesnoy, S.; Huang, L. *Annu Rev. Biophys. Biomol. Struct.* **2000**, *29*, 27.
(16) Ahmad, A.; Evans, H. M.; George, C. X.; Samuel, C. E.; Safinya, C. R. J. *Gene Med.* **2005**, *7*, 739.
(17) Koiv, A.; Palvimo, J.; Kinnunen, P. K. J. *Biochemistry* **1995**, *34*, 8018.
(18) Chonn, A.; Cullic, P. R.; Devine, D. V. *J. Immunol*. **1991**, *146*, 4234.
(19) Tardi, P. G.; Boman, N. L.; Cullis, P. R. *J. Drug Targeting* **1996**, *4*, 129.
(20) Francescangeli, O.; Stanic, V.; Gobbi, L.; Bruni, P.; Iacussi, M.; Tosi, G.; Bernstorff, S. *Phys. Rev. E* **2003**, *67*, 011904.
(21) Francescangeli, O.; Pisani, M.; Stanic, V.; Bruni, P.; Iacussi, M. *Recent Res. Dev. Macromol. Res.* **2003**, *7*, 247.
(22) Francescangeli, O.; Stanic, V.; Lucchetta, D.; Bruni, P.; Iacussi, M.; Cingolani, F. *Mol. Cryst. Liq. Cryst.* **2003**, *398*, 259.
(23) Caracciolo, G.; Sadun, C.; Caminiti, R.; Pisani, M.; Bruni, P.; Francescangeli, O. *Chem. Phys. Lett*. **2004**, *397*, 138.
(24) Pisani, M.; Bruni, P.; Conti, C.; Giorgini, E.; Francescangeli, O. *Mol. Cryst. Liq. Cryst*. **2005**, *434*, 643.
(25) Bruni, P.; Pisani, M.; Iacussi, M.; Francescangeli, O. *Org. Biomol. Chem*. **2005**, *3*, 3524.
(26) Francescangeli, O.; Pisani, M.; Stanic, V.; Bruni, P.; Weiss, T. M. *Europhys. Lett*. **2004**, *67*, 669.
(27) Bruni, P.; Pisani, M.; Amici, A.; Marchini, C.; Montani, M.; Francescangeli, O. *Appl. Phys. Lett*. **2006**, *88*, 073901.
(28) Ruocco, M. J.; Shipley, G. G. *Biochim. Biophys. Acta* **1982**, *691*, 309.
(29) Sun, W. J.; Tristram-Nagle, S.; Suter, R. M.; Nagle, J. F. *Biophys. J*. **1996**, *71*, 885.
(30) Nagle, J. F.; Zhang, R.; Trsistram-Nagle, S.; Sun, W.; Petrache, H. I.; Suter, R. M. *Biophys. J.* **1996**, *70*, 1419.
(31) Mason, P. C.; Gaulin, B. D.; Epand, R. M.; Wignall, G. D.; Lin, J. S. *Phys. Rev. E* **1989**, *40*, 2712.
(32) McManus, J. J.; Rädler, J. O.; Dawson, K. A. *J. Phys. Chem. B* **2003**, *107*, 9869.
(33) McManus, J. J.; Rädler, J. O.; Dawson, K. A. *Langmuir* **2003**, *19*, 9630.
(34) McManus, J. J.; Rädler, J. O.; Dawson, K. A. *J. Am. Chem. Soc*. **2004**, *26*, 15966.

(35) Francescangeli, O.; Rinaldi, D.; Laus, M.; Galli, G.; Gallot, B. *J. Phys. II* **1996**, *6*, 7 and references therein.
(36) Tristram-Nagle, S.; Petrache, H. I.; Nagle, J. F. *Biophys. J*. **1998**, *75*, 917.
(37) Worthington, C. R.; Khare, H. I. *Biophys. J.* **1978**, *23*, 407.
(38) Nagle, J. F.; Tristram-Nagle, S. *Biochim. Biophys. Acta* **2000**, *1469*, 159.
(39) Winter, I.; Pabst, G.; Rappolt, M.; Lohner, K. *Chem. Phys. Lipids* **2001**, *112*, 137.
(40) Kharakoz, D. P.; Khusainova, R. S.; Gorelov, A. V.; Dawson, K. A. *FEBS Lett*. **1999**, *446*, 27.
(41) Nichols, P.; Miller, N. *Biochim. Biophys. Acta* **1974**, *356*, 184.
(42) Chapman, D.; Peel, W. E.; Kingston, B.; Lilley, T. H. *Biochim. Biophys. Acta* **1977**, *464*, 260.
(43) Tatulian, S. A. *Eur. J. Biochem*. **1987**, *170*, 413.
(44) Wack D. C.; Webb, W. W. *Phys. Rev. A* **1989**, *40*, 2712.
(45) Hentschel M. P.; Rustichelli, F. *Phys. Rev. Lett*. **1991**, *66*, 903.
(46) Rappolt, M.; Pabst, G.; Rapp, G.; Kriechbaum, M.; Amenitsch, H.; Krenn, C.; Bernstorff, S.; Laggner, P. *Eur. Biophys. J.* **2000**, *29*, 125.
(47) Sun, W. J.; Suter, R. M.; Knewtson, M. A.; Worthington, C. R.; Tristram-Nagle, S.; Zhang, R.; Nagle, J. F. *Phys. Rev. E* **1994**, *49*, 4665.
(48) Tardieu A.; Luzzati, V. *J. Mol. Biol.* **1972**, *75*, 711.
(49) Craievich, A. F.; Levelut, A. M.; Lambert, M.; Albon N. *J. Phys*. **1978**, *39*, 377.
(50) Rouzina I.; Bloomfield, V. A. *J. Phys. Chem*. **1996**, *100*, 9977.
(51) Smith, G. S.; Sirota, E. B.; Safinya, C. R.; Plano, R. J.; Clark, N. A. *J. Chem. Phys*. **1990**, *92*, 4519.
(52) Zantl, R.; Artzner, F.; Rapp, G.; Radler, J. O. *Europhys. Lett*. **1998**, *45*, 90.
(53) Zantl, R.; Baicu, L.; Artzner, F.; Sprenger, I.; Rapp, G.; Radler, J. O. *J. Phys. Chem. B* **1999**, *103*, 10300.
(54) Stadler, J.; Lemmens, R.; Nyhammar, T. *J. Gene Med*. **2004**, *6*, S1, 54.